ELUCIDATING THE DESIGN SPACE OF FP4 TRAINING

Anonymous authors
Paper under double-blind review

ABSTRACT

The increasing computational demands of foundation models have spurred research into low-precision training, with 4-bit floating-point (FP4) formats emerging as a frontier for maximizing hardware throughput. While numerous techniques have been proposed to stabilize FP4 training, they often present isolated solutions with varying, and not always clear, computational overheads. This paper aims to provide a unified view of the design space of FP4 training. We introduce a comprehensive, quantisation gradient-based framework for microscaling quantization that allows for a theoretical analysis of the computational costs associated with different stabilization methods on both the forward and backward passes. Using a simulator built on this framework, we conduct an extensive empirical study across a wide range of machine learning tasks, including regression, image classification, diffusion models, and language models. By systematically evaluating thousands of combinations of techniques—such as novel gradient approximations, rounding strategies, and scaling methods, we identify which configurations offer the most favourable performance-to-overhead trade-off. We find that the techniques enabling the best trade-off involve carefully combining Hadamard transformations, tensor scaling and stochastic rounding. We further find that using UE5M3 as a scaling factor potentially offers a good compromise between range and precision with manageable computational overhead.

1 INTRODUCTION

With the emergence of foundation models (Bommasani et al., 2021), the demand for computational resources has grown proportionally to the parameter count of these models, which often span from billions to trillions of parameters. Many of these models rely on the transformer architecture (Vaswani et al., 2017), which is ubiquitous across vision, text and video models (Khan et al., 2022). These models tend to be compute bound by two operations: the attention mechanism (Duman-Keles et al., 2023; Dolga et al., 2024) which tends to scale quadratically with sequence length, and the matmul operations from the weight matrices (Corp, 2025) which are quadratic with respect to size of the hidden dimensions.

In this paper, we conduct the first large-scale, systematic investigation of the FP4 design space. Traditionally, machine learning training uses FP32 format which serves as the baseline with the highest accuracy and lowest throughput. Historically, with each subsequent generation of hardware, the precision has been halved — starting from FP16 (Micikevicius et al., 2018), FP8 (Noune et al., 2022; Micikevicius et al., 2022; Fishman et al., 2025), and now FP4 (Tseng et al., 2025; Chen et al., 2025; Castro et al., 2025; Hao et al., 2025; Chmiel et al., 2025; Wang et al., 2025; Yang et al., 2025; Su et al., 2025; Li et al., 2025; Cao et al., 2025). Halving the precision often allows a doubling of the throughput for matrix multiplication operations (Hao et al., 2025), hence with each iteration careful adjustments need to be made to the training procedure to account for the loss of numerical accuracy.

While these works introduce new techniques to stabilize FP4 training for larger models, they all propose different methodologies with varying computational overhead that are empirically shown to work in isolation through simulations in BFLOAT16. However, a systematic evaluation of the performance-overhead trade-offs has been missing. As an example, Wang et al. (2025) introduces a quantile based pruning and gradient adjustment, both of which are shown to be useful, however both add an additional $\sim \mathcal{O}(n)$ time and memory overhead which cannot be done in low-precision and is non-fusable. It should be further noted that the simulation procedure in Wang et al. (2025) does not adequately quantise the scale, which their description implies is kept in high-precision – a detail

that can significantly impact training stability. Similarly, Tseng et al. (2025) proposes a block-wise Hadamard transformation, which induces a $\sim \mathcal{O}(n \log l)$ overhead. It should be noted that none of the aforementioned papers simulate FP4 training fully, as Wang et al. (2025) only consider quantising weights and activations and not the gradient and Tseng et al. (2025) only quantises the gradient. Further, Cao et al. (2025); Li et al. (2025) proposes spectral decomposition techniques to handle outliers, which consequently introduces $\mathcal{O}(nk)$ time and $\mathcal{O}(k^2)$ memory, which in terms of hardware acceleration is also non-fusable. It is currently not clear whether these additional overheads are necessary in downstream implementations of low-precision matrix multiplication, as some evidence in Chmiel et al. (2025); Yang et al. (2025) suggests that something as simple as *Stochastic Rounding (SR)* is enough to stabilise FP4 training. Here l denotes block size, n denotes number of elements in the tensor and k the low-rank projection dimension in SVD.

The goal of this work is to develop a thorough understanding of the quantisation mechanism and how it affects the training procedure and illuminate which techniques offer a worthwhile trade-off in terms of additional overhead vs performance benefit. We summarise the contributions of this paper as follows:

1. We propose a quantisation gradient-based framework for FP4 quantisation, which is used to derive the computational overhead of conceivably useful techniques (both novel and existing ones) on the forward and backward pass of a quantised linear layer.
2. We implement the framework as a simulator [1] , running experiments of across various machine learning tasks to gain insight on which combination of techniques offer a reasonable overhead vs. performance benefit.

We first introduce our unified, gradient-based framework in Section 2, then use it to analyze the design space of scaling, rounding, and gradient approximation techniques in Sections 3, 4, and 5. We survey other relevant methods in Section 6, present our extensive empirical validation in Section 7, and conclude with our key findings.

2 A COMMON FRAMEWORK FOR FP4 TRAINING

In this section, we detail what happens when we use microscaling formats to quantize a tensor for a linear layer forward pass. Consider a tensor $\mathbf{X} \in \mathbb{R}^{m \times n}$. We first define $\mathbf{X}$ represented in microscaling format Rouhani et al. (2023).

Definition 1. *A* micro-scaled block *is defined by a scalar $s \in \mathbb{R}$ and a vector $\mathbf{P} = [p_i]_{i=1}^{l}$ of l elements. Each value x_i can be recovered as*

$$x_i = s \cdot p_i.$$

The parameter l is a fixed constant known as the block size*. Given a tensor $\mathbf{X} \in \mathbb{R}^{m \times n}$ and a block size of l, the* MX representation *of $\mathbf{X}$ consists of a collection of tuples*

$$\{(s_j, \mathbf{P}_j)\}_{j=1}^{(m \cdot n)//l},$$

where each tuple corresponds to a block of l elements in $\mathbf{X}$.

Intuitively, microformat scaling represents partitions of a tensor with a common scale often used to normalise the partition, where the scaled elements $\mathbf{P}_j$ is quantized to a lower precision. We formally detail the quantisation procedure for one partition $\mathbf{X}_p \in \mathbb{R}^l$ below, represented by a transformation f:

$$f(\mathbf{X}_p) = \frac{1}{s_q} Q(s_q \cdot \mathbf{X}_p)$$

where the components are defined as follows:

Outer Scaling Factor (s_q): This factor is a function of $\mathbf{X}_p$. First, an intermediate factor $s(\mathbf{X}_p)$ is computed:

$$s(\mathbf{X}_p) = \frac{\texttt{FP4 max}}{Z(\mathbf{X}_p)}$$

[1] Codebase: Google Drive Link

Here, $Z : \mathbb{R}^l \to \mathbb{R}$ is a scalar-valued function of the tensor $\mathbf{X}_p$ (e.g., the absolute maximum norm, `absmax`). This factor is then quantized:

$$s_q = q(s(\mathbf{X}_p))$$

Quantization Function (Q): Q is an element-wise function that quantizes the elements of $\mathbf{X}_p$.

We can now introduce the gradient with respect to an element in $\mathbf{X}$:

Proposition 1. *Let $f(\mathbf{X}_p) = \frac{1}{s_q} Q(s_q \cdot \mathbf{X}_p)$ Then, the partial derivative of f_{ij} with respect to $\mathbf{X}_{ij}$, that is the diagonal of the Jacobian matrix, is given by:*

$$\boxed{\frac{\partial f_{ij}}{\partial \mathbf{X}_{ij}} = Q'(s_q \mathbf{X}_{ij}) + \frac{\partial s}{\partial \mathbf{X}_{ij}} \left[\frac{q'(s)}{s_q} \left(\mathbf{X}_{ij} Q'(s_q \mathbf{X}_{ij}) - \frac{1}{s_q} Q(s_q \mathbf{X}_{ij}) \right) \right]} \tag{1}$$

See Appendix A.7 for derivations.

In the context of a linear layer with weights $\mathbf{W} \in \mathbb{R}^{n \times m}$ and input data $\mathbf{X} \in \mathbb{R}^{b \times m}$, the output $\mathbf{Y} = f(\mathbf{X}) f(\mathbf{W})^\top$ would have the corresponding gradients:

$$\frac{\partial \mathcal{L}}{\partial \mathbf{X}} = \left(\frac{\partial \mathcal{L}}{\partial \mathbf{Y}} \cdot f(\mathbf{W}) \right) \odot \frac{\partial f(\mathbf{X})}{\partial \mathbf{X}}, \quad \frac{\partial \mathcal{L}}{\partial \mathbf{W}} = \left(\left(\frac{\partial \mathcal{L}}{\partial \mathbf{Y}} \right)^\top \cdot f(\mathbf{X}) \right) \odot \frac{\partial f(\mathbf{W})}{\partial \mathbf{W}}.$$

Here, $\mathcal{L}$ denotes the scalar loss, $\odot$ the elementwise product and $f(\cdot)$ is a differentiable transformation (e.g., MX decomposition or quantization-aware mapping) applied to the inputs and weights. In the next section, we detail different choices in terms of calculating and approximating $\frac{\partial \mathcal{L}}{\partial \mathbf{X}}, \frac{\partial \mathcal{L}}{\partial \mathbf{W}}$. We summarise the time and memory overhead of our proposed and existing techniques in Table 2.

3 TENSOR SCALING IN FP4 TRAINING

An alternative to applying block-wise scaling directly is to first normalize the entire tensor Blake et al. (2023); Micikevicius et al. (2022); Sun et al. (2019); Peng et al. (2023). The goal of this strategy is to improve the quantization of the scaling factors themselves. In this approach, a tensor-wise scaling factor g is computed, used to normalize the tensor, and then multiplied back after the block-wise quantization. While the intent is for g to cancel out, the non-linear nature of the scale quantization function $q(\cdot)$ results in a distinct final transformation.

Let $g = \max_p \{m_p\}, \quad m_p = Z(\mathbf{X}_p)$ be the global scaling factor for a tensor $\mathbf{X}$, and let $\mathbf{U} = \mathbf{X}/g$ be the globally normalized tensor. The transformation $h(\mathbf{X})$ for an element $\mathbf{X}_{ij}$ within a block p is defined as $h_{ij}(\mathbf{X}_p) = g \cdot f_{ij}(\mathbf{U}_p)$.

Here, $f(\mathbf{U}_p)$ is the block-wise quantization function from Section 2 applied to the normalized block $\mathbf{U}_p$. Its components are functions of $\mathbf{U}_p$:

1. **Ideal Scale:** $s'_p = \frac{\text{FP4}_{\max}}{Z(\mathbf{U}_p)} = g \cdot \frac{\text{FP4}_{\max}}{Z(\mathbf{X}_p)} = g \cdot s_p$
2. **Quantized Scale:** $s'_{q,p} = q(s'_p) = q(g \cdot s_p)$

Substituting these gives the full forward pass expression for an element:

$$\boxed{h_{ij}(\mathbf{X}) = \frac{g}{q\left(g \cdot s_p\right)} Q\left(q(g \cdot s_p) \cdot \frac{\mathbf{X}_{ij}}{g} \right)} \tag{2}$$

The gradient of this transformation accounts for both the block-wise dependencies and the global dependency on g.

Corollary 1. *Let $h(\mathbf{X})$ be the quantization with intermediate global normalization. For an element $\mathbf{X}_{ij}$ in block p, the partial derivative is:*

$$\boxed{\frac{\partial h_{ij}}{\partial \mathbf{X}_{ij}} = \frac{\partial f_{ij}}{\partial \mathbf{U}_{p,ij}} + \frac{\partial g}{\partial \mathbf{X}_{ij}} \left(f_{ij}(\mathbf{U}_p) - \mathbf{U}_{p,ij} \frac{\partial f_{ij}}{\partial \mathbf{U}_{p,ij}} \right)} \tag{3}$$

where $\frac{\partial f_{ij}}{\partial \mathbf{U}_{p,ij}}$ is the full gradient from the first Theorem, evaluated on the normalized block $\mathbf{U}_p$ with its corresponding scales ($s'_p, s'_{q,p}, k'_p$). See Appendix A.8 for derivations.

It should be noted that g in context of the MXFP4(FP4 format with E8M0 scale) and NVFP4 (FP4 format with E4M3 scale) has overhead complexity $\mathcal{O}((m \cdot n)//l)$ as opposed to $\mathcal{O}(m \cdot n)$ when computing $\texttt{absmax}(\mathbf{X})$, since it suffices to search the scales rather than the entire tensor $\mathbf{X}$.

3.1 Rounding and Scaling Strategies

Recent work in low-precision training has highlighted that the rounding strategy for scaling factors can have a profound impact on model stability. For instance, Mishra et al. (2025) found that for MXFP8 formats, rounding-to-positive-infinity improves signal propagation by reducing the number of saturated values, given the limited range of the scaling factor. As our work considers both E4M3 (which has a limited range) and E8M0 (which has a wider range), we evaluate both round-to-nearest (RTN) and round-to-positive-infinity in our experiments.

We note that the results in Chmiel et al. (2025) get NVFP4 to converge without any issues with tensor scaling, as they mitigate any overflow by taking $\tilde{s}_p = \frac{s'_p}{\texttt{FP4}_{\max} \cdot \texttt{E4M3}_{\max} \cdot 0.5}$. This pushes down the effective range of $\tilde{s}_p \in [2/\texttt{E4M3}_{\max}, 2/\texttt{E4M3}_{\max} \cdot g)$. While not completely protected from overflow, it's a good rule of thumb to maximize the utilised range of E4M3. We use this technique when applying tensor scaling for NVFP4. We note that this heuristic can be extended to any scale format beyond E4M3, as it effectively rescales the scale factor to utilise its maximum range.

Handling Zero-Valued Scales. A critical edge case is the handling of zero-valued scaling factors, resulting in division by zero in the dequantisation. Chmiel et al. (2025) replaces any zero scale with one, which may induce further quantisation errors as small scales are set to 1. We propose rounding the zeros and underflows to the closest representable subnormal value in the target format and saturate overflows to the maximum representable number. We compare the efficacy of both approaches in our experiments.

Rounding of the weight tensor The impact of the rounding strategy has previously been demonstrated (Chmiel et al., 2025; Fitzgibbon & Felix, 2025) to have significant impact on the stability of LLM training in low-precision formats. The main observations for FP4 formats is to use *round-to-nearest* (RTN) for the forward pass and *stochastic rounding* (SR) in the backwards pass (Chmiel et al., 2025; Yang et al., 2025), specifically on the activation and gradient tensors. We follow the quantisation procedure in Rouhani et al. (2023), which considers 6 quantisations for a forward and backward pass in a linear layer. We benchmark against the strategy proposed by Chmiel et al. (2025) and additionally consider SR on the activations in the forward pass as well.

Rounding of the scales We also experiment with stochastic rounding in the scaling factor as well. We motivate this design choice with the observation that E8M0 has very large intervals between each number, leading to potential bias, which can mitigated more effectively at the scaling factor.

4 Differentiable Relaxations for Quantization

Approximating $Q'(\mathbf{X})$ and $q'(x)$ Wang et al. (2025) take $\frac{\partial f_{ij}}{\partial \mathbf{W}_{ij}} \approx Q'(s \cdot \mathbf{W}_{ij})$. However since Q is a quantisation function which is not differentiable, they approximate $Q(x) \approx \frac{\delta}{2} \cdot \left(1 + \text{sign}\left(\frac{2x}{\delta} - 1\right) \cdot \left|\frac{2x}{\delta} - 1\right|^{\frac{1}{w}}\right)$, with gradient $Q'(x) = \frac{1}{w} \cdot \left|\frac{2x}{\delta} - 1\right|^{\frac{1}{w}-1}$. They propose $w = 5$ in their implementation. There are some potential flaws with the proposed parametrisation, as calculating power of fractionals tends to be computationally expensive and require $\mathcal{O}(w)$ cycles. This leads to the overall complexity of $\mathcal{O}(nmw \log_2(k))$, where $\log(k)$ comes from finding the interval on the E2M1 grid to which x belongs using binary search, with k being the grid size. We thus propose an alternative differentiable relaxation of $Q(x)$.

Linear Spline approximation A linear spline is a continuous piecewise linear function defined over a set of sorted knots $t_0, \ldots, t_n$. These knots partition the domain into n intervals $I_i = [t_i, t_{i+1})$. The function's continuity is ensured by having the linear segments connect at the knots.

The forward and backward passes evaluate the spline and its derivative. For an input $x \in [t_i, t_{i+1})$, the spline is a line segment, $S(x) = a_i(x - t_i) + b_i$ (**Forward pass**) with $S'(x) = a_i$ (**Backward pass**). Here, b_i represents the value of the spline at knot t_i (i.e., $S(t_i)$), and a_i is the slope of the line segment over the interval $[t_i, t_{i+1})$.

We illustrate our proposed differentiable quantization approximation and its corresponding gradient in Fig. 1. The function is shown in Fig. 1a, and its gradient is depicted in Fig. 1b. We found that applying the quantisation gradient in the backwards pass sometimes would mask out the gradient entirely, hence we propose clipping $Q'(x)$ from below to prevent multiplying the gradient with 0 (Figure 1c). The overall complexity overhead of the spline approximation is thus $\mathcal{O}(nm \log_2(k))$.

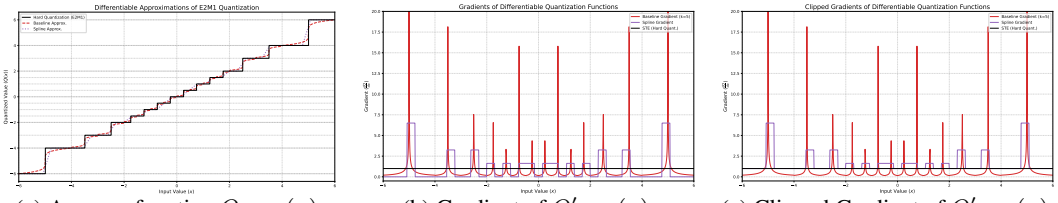

(a) Approx. function $Q_{\text{approx}}(x)$. (b) Gradient of $Q'_{\text{approx}}(x)$. (c) Clipped Gradient of $Q'_{\text{approx}}(x)$.

Figure 1: Approximations of $Q(x)$ and their corresponding gradients, assuming ties-to-even rounding. We refer to Wang et al. (2025) as the baseline.

Note that we need to save the unquantised matrix $\mathbf{X}$ for the backwards pass to evaluate $Q'(\mathbf{X})$, adding $\mathcal{O}(mn)$ memory overhead.

5 Gradient Adjustment for Scaling Factor Quantization

The gradient adjustment techniques used for weights and activations can also be applied to the quantization of the scaling factor $q(s)$. However, the relatively high dynamic range required for scaling factors introduces additional complexity. To find a decent trade-off between accuracy and complexity, we first analyze the regions where the quantization error is most significant. We measure this error using the relative deviation, defined as the ratio s/s_q. A value of this ratio far from 1 indicates a large quantization error.

Figure 2 illustrates the quantization functions for the `E4M3` and `E8M0` scale formats and their corresponding relative deviations. The quantization function itself is shown in Fig. 2a, while the error is plotted in Fig. 2b.

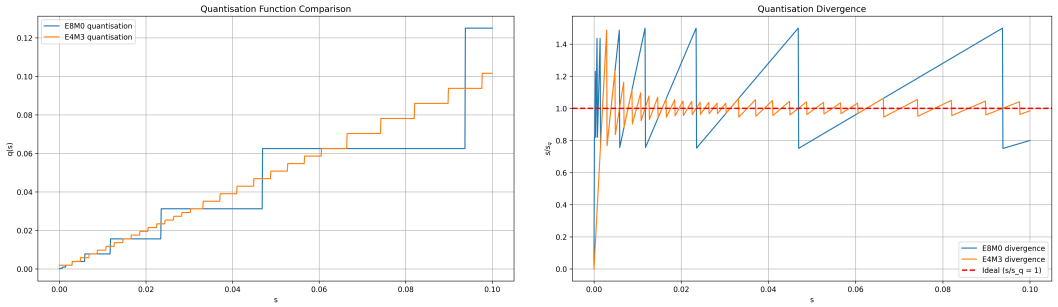

(a) Quantization functions $s_q = q(s)$. (b) Relative deviation s/s_q.

Figure 2: Comparison of quantization for `E4M3` and `E8M0` scaling factors. Figure (a) shows the quantization step functions. Figure (b) shows the relative deviation, which is most pronounced for small values of the scaling factor s.

As illustrated in Fig. 2b, the largest relative deviation occurs for small-magnitude scaling factors, especially within the first few representable values of the `E4M3` scale format. Based on this observation, we can choose to apply the gradient adjustment selectively, targeting only the range where the quantization error is highest when computing the $q'(s)$ term.

5.1 Gradient Adjustment of absmax: Adjusting for $Z(\mathbf{X}_p)$ and $s'(\mathbf{X}_p)$

First, we establish the general relationship between the gradient of the scaling factor, $\frac{\partial s}{\partial \mathbf{X}}$, and the gradient of the normalization function, $\frac{\partial Z}{\partial \mathbf{X}}$.

Proposition 2. *Given the scaling factor* $s(\mathbf{X}) = \frac{\texttt{FP4 max}}{Z(\mathbf{X})}$*, its gradient with respect to an element* $\mathbf{X}_{ij}$ *is given by:*

$$\frac{\partial s}{\partial \mathbf{X}_{ij}} = -\frac{\texttt{FP4 max}}{Z(\mathbf{X})^2}\frac{\partial Z}{\partial \mathbf{X}_{ij}}$$

See Appendix A.9 for derivations.

The following corollaries provide the specific form of this gradient for two common choices of the normalization function $Z(\mathbf{X})$.

Corollary 2. *If the normalization function* $Z(\mathbf{X})$ *is* `absmax`*,* $Z(\mathbf{X}) = \max_{k,l} |\mathbf{X}_{kl}|$*, then the gradient of the scaling factor is non-zero only for the element with the maximum absolute value:*

$$\frac{\partial s}{\partial \mathbf{X}_{ij}} = -\frac{\texttt{FP4 max}}{Z(\mathbf{X})^2}\left(\text{sign}(\mathbf{X}_{i^*j^*}) \cdot \delta_{ii^*}\delta_{jj^*}\right) \tag{4}$$

where (i^*, j^*) *is the index of the maximum absolute value element and* δ *is the Kronecker delta. See Appendix A.10 for derivations.*

Corollary 3. *If the normalization function* $Z(\mathbf{X})$ *is the smooth LogSumExp approximation of the max function,* $Z(\mathbf{X}) = \frac{1}{\beta}\log\left(\sum_{k,l} e^{\beta|\mathbf{X}_{kl}|}\right)$*, the gradient of the scaling factor is a dense gradient given by:*

$$\frac{\partial s}{\partial \mathbf{X}_{ij}} = -\frac{\texttt{FP4 max}}{Z(\mathbf{X})^2}\left(\text{softmax}(\beta|\mathbf{X}|)_{ij} \cdot \text{sign}(\mathbf{X}_{ij})\right) \tag{5}$$

See Appendix A.11 for derivations.

We consider four configurations for calculating the gradients with respect to the scaling factors, summarized in Table 1. Alongside the standard 'Absmax' and 'Softmax' approaches, we introduce a 'Hybrid' method. This approach uses the computationally efficient 'absmax' function in the forward pass but approximates its gradient with the dense 'softmax' derivative during the backward pass. This is intended to propagate gradient information to more elements without incurring the forward-pass cost of the LogSumExp operation.

Table 1: Gradient configurations for the block-wise scale $s(\mathbf{X})$ and global scale $g(\mathbf{X})$. The Straight-Through Estimator (STE) gradient is a heuristic approximation, as detailed in the text.

Configuration	**Scaling Function** $Z(\mathbf{X})$	**Gradient** $\frac{\partial s}{\partial \mathbf{X}_{ij}}$	**Global Scaling Function** $g(\mathbf{X})$	**Gradient** $\frac{\partial g}{\partial \mathbf{X}_{ij}}$
STE	$\max_{k,l}\|\mathbf{X}_{kl}\|$	1	$\max_{k,l}\|\mathbf{X}_{kl}\|$	1
Absmax	$\max_{k,l}\|\mathbf{X}_{kl}\|$	$-\frac{\texttt{FP4 max}}{(Z(\mathbf{X}))^2}\left(\text{sign}(\mathbf{X}_{i^*j^*}) \cdot \delta_{ii^*}\delta_{jj^*}\right)$	$\max_{k,l}\|\mathbf{X}_{kl}\|$	$\text{sign}(\mathbf{X}_{i^*j^*}) \cdot \delta_{ii^*}\delta_{jj^*}$
Softmax	$\frac{1}{\beta}\log\left(\sum_{k,l} e^{\beta\|\mathbf{X}_{kl}\|}\right)$	$-\frac{\texttt{FP4 max}}{(Z(\mathbf{X}))^2}\left(\text{softmax}(\beta\|\mathbf{X}\|)_{ij} \cdot \text{sign}(\mathbf{X}_{ij})\right)$	$\frac{1}{\beta}\log\left(\sum_{k,l} e^{\beta\|\mathbf{X}_{kl}\|}\right)$	$\text{softmax}(\beta\|\mathbf{X}\|)_{ij} \cdot \text{sign}(\mathbf{X}_{ij})$
Hybrid	$\max_{k,l}\|\mathbf{X}_{kl}\|$	$-\frac{\texttt{FP4 max}}{(Z(\mathbf{X}))^2}\left(\text{softmax}(\beta\|\mathbf{X}\|)_{ij} \cdot \text{sign}(\mathbf{X}_{ij})\right)$	$\max_{k,l}\|\mathbf{X}_{kl}\|$	$\text{softmax}(\beta\|\mathbf{X}\|)_{ij} \cdot \text{sign}(\mathbf{X}_{ij})$

For any softmax-based configuration, we must either compute or save the softmax for the backwards pass, incurring additional time and memory complexity. For *Absmax*, it suffices to save the index of the maximum value. For the STE case of $\frac{\partial s}{\partial \mathbf{X}_{ij}}$, we are effectively setting the entire second term from Equation (1), $\left[\frac{q'(s)}{s_q}\left(\mathbf{X}_{ij}Q'(s_q\mathbf{X}_{ij}) - \frac{1}{s_q}Q(s_q\mathbf{X}_{ij})\right)\right]$, to be equal to 1. This provides a simple alternative to completely omit the $\mathcal{O}(3mn)$ extra computation of this extra gradient term, treating the complex scaling derivative as a direct pass-through. We have an `ignore` option for the $\frac{\partial g}{\partial \mathbf{X}_{ij}}$ term, which means setting the corresponding update term from Corollary 1 to zero: $\frac{\partial g}{\partial \mathbf{X}_{ij}}\left(f_{ij}(\mathbf{U}_p) - \mathbf{U}_{p,ij}\frac{\partial f_{ij}}{\partial \mathbf{U}_{p,ij}}\right) = 0$, skipping the extra $\mathcal{O}(4mn)$ work and saving memory.

6 Other techniques

Optimizer centric Recently, Huang et al. (2025) proposed StableSPAM, which modifies the Adam optimiser by bounding the momentum term with a moving average statistic. This is motivated by the

Table 2: Summary of FP4 Training Techniques and Overheads. Here we assume each operation is applied to a tensor with n elements, which can be partitioned to n/l blocks with block size l.

Technique	Compute Overhead	Additional Memory	Fuseability	Comment
Straight-Through Estimator (STE)	$\mathcal{O}(1)$	None	Yes	
Baseline $Q'(\mathbf{X})$(Wang et al., 2025)	$\mathcal{O}(n \cdot w \log k)$	$\mathcal{O}(n)$	No	$w = 5$
Spline $Q'(\mathbf{X})$	$\mathcal{O}(n \log k)$	$\mathcal{O}(n)$	No	
Stochastic Rounding (Fitzgibbon & Felix, 2025)	$\mathcal{O}(n)$	None	Yes	
Stochastic Rounding Scale	$\mathcal{O}(n//l)$	None	Yes	
Global Tensor Scaling (Blake et al., 2023)	$\mathcal{O}(n)$	$\mathcal{O}(1)$	Yes	Rescale in full prec.
Global Scaling Gradient (Corollary 1)	$\mathcal{O}(3n)$	$\mathcal{O}(3n)$	No	Save ex. tensor
Differentiable Scale (Absmax)	$\mathcal{O}(4n)$	$\mathcal{O}(3n)$	No	
Differentiable Scale (Softmax)	$\mathcal{O}(4n)$	$\mathcal{O}(4n)$	No	Softmax backw.
Scale Gradient Adjustment	$\mathcal{O}(n)$	$\mathcal{O}(n//l)$	No	Only for Diff. Scale
Outlier concentration (Hadamard) (Tseng et al., 2025)	$\mathcal{O}(n \cdot \log l)$	None	Yes	On-the-fly possible
StableSPAM Optimizer (Huang et al., 2025)	$\mathcal{O}(n)$	$\mathcal{O}(1)$	No	
Dynamic Loss Scaling (Micikevicius et al., 2018)	$\mathcal{O}(n)$	$\mathcal{O}(1)$	No	Mult. each tensor
SVD techniques (Li et al., 2025; Cao et al., 2025)	$\mathcal{O}(nk)$	$\mathcal{O}(k^2)$	No	

observation that in low precision, the gradient norms tend to explode during training, meaning more careful normalisation of the momentum norm and bounding of large values is needed to stabilise training. While their optimiser is primarily tailored around LLMs, we explore the impact of combining StableSPAM with existing rounding and gradient adjustment based techniques for general purpose ML workloads.

Loss scaling We consider loss scaling as a technique to propagate signal when the range of the precision is very limited following Micikevicius et al. (2018). We implement the automated loss scaling technique, which adjusts the loss scaling scale dynamically during training.

Outlier concentration During quantisation, outliers in high-precision may induce quantisation error as they impact the scaling during quantisation. Recent work by Tseng et al. (2024; 2025) proposes applying $Q(\mathbf{HSX}_p)$ to concentrate outliers towards the median of the data. Here $\mathbf{HS}$ is the random Hadamard transform applied to each block $\mathbf{X}_p$ of size l elements, inducing a $\mathcal{O}(\frac{mn}{l} l \cdot \log(l))$ compute overhead. It should be noted that this operation is fusable, and can be done on-the-fly with warp shuffle operations. We consider applying Hadamard transformation in both the forward and backward pass and only the backward pass, akin to Tseng et al. (2024; 2025); Castro et al. (2025).

Spectral decomposition In Li et al. (2025); Cao et al. (2025), they propose to use spectral decomposition techniques to alleviate the difficulty of quantising outliers in low-precision. This is done by decomposing the tensor into a low-rank representation using *singular value decomposition* (SVD), where the low-rank components are then quantised instead. As this is non-fusable, and has prohibitive time complexity overhead $\mathcal{O}(mnk)$ (with k referring to a chosen lower rank), we do not consider it for our simulations as the Hadamard transformation offers a more seamless alternative in the pre-training setting.

7 Experiments

Experimental design and selection strategy We consider the search space in Appendix Table 10, which totals to over 20,000 different parameter combinations, an infeasible search space for larger models. Consequently, our strategy is to do larger sweeps for smaller models that are faster to train and using the results to derive insights and prune the search space for larger models. We run the experiments in the order described in Appendix Table 11.

Performance–efficiency score We define an efficiency score $S(c) = \frac{G(c)}{1+\Omega(c)}$, for a configuration c, that balances relative performance gain $G(c) = (M_{\text{ref}} - M_c)/M_{\text{ref}}$ against a complexity penalty $\Omega(c) = \sum_{t \in \mathcal{T}_c} w_t$. Here, $\mathcal{T}_c$ is the set of non-standard techniques used, w_t their overhead points, and the $+1$ ensures a well-defined score for baseline configurations. Scores are split by positive/negative gain per format, guiding pruning toward configurations that maximize performance with minimal added complexity (see Appendix A.6 for more details). We consider validation loss for M when we calculate the score.

7.1 RESULTS

Loss curves of ImageNet-100, Gaussian regression, U-net large (big_diffusion) and Llama 60M, 350M and 1B are in Figure 3. For detailed results of each dataset we refer to Appendices A.2 and A.5. Based on our learnings from experiments, we present three guiding principles when training in FP4.

Figure 3: Training and validation performance curves for selected models and datasets.

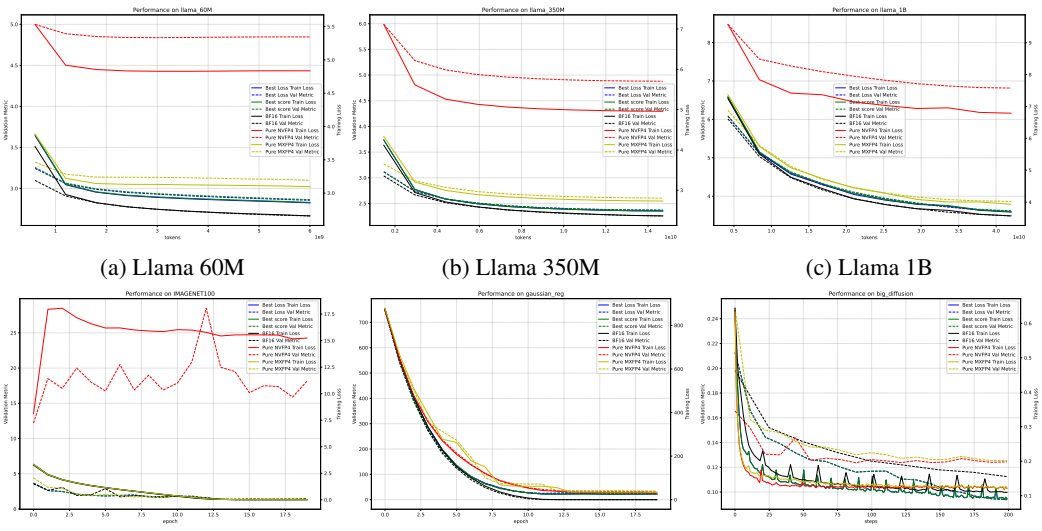

(a) Llama 60M (b) Llama 350M (c) Llama 1B

(d) ImageNet-100 (e) Gaussian Reg. (f) Big Diffusion

Principle 1: Gradient Stability Outweighs Unbiasedness Across all our experiments (Appendix A.2) we found that none of the proposed gradient adjustment had any significant positive effect on training stability compared to STE and consequently we were unable to match the findings in Wang et al. (2025). As a possible explanation for this, consider the `absmax` gradient (Corollary 2), which is a single non-zero entry per block. This mathematically enforces a sparse, high-variance update signal that may introduce high-variance, impacting momentum based optimisers such as Adam or StableSPAM. We also observed this when experimenting with $Q'(\mathbf{X})$, that adding this gradient without lower and upper bound clipping of the relaxation (see Figure 1c) ended up masking out the downstream signal. Consequently using STE, which offers a dense and stable update and led to more stable training in the low-precision context.

Principle 2: Scale Representation is the Primary Bottleneck We find throughout our experiments and ablations studies that the range of the scaling factor has a profound effect on training stability, especially demonstrated in larger language models and the ImageNet-100 runs in Appendix Tables 3 and 4. As many of our results contradicted findings in Chmiel et al. (2025), we ran ablation studies in Appendix A.3 investigating the additional impact of `SmoothSwiGLU`[2] (Fishman et al., 2025) on language models and ablating the range of `E4M3` scaling, by replacing it with `E8M3` in Appendix A.4. Our findings suggest that `E4M3`, despite applying tensor scaling, did not converge due to its range limitation. We speculate that a potential sweet spot exists between `E8M0` and `E4M3`. We then experiment with `UE5M3` in Appendix A.5, a format that has increased range and additional precision and find that it indeed consistently outperforms `E8M0` on language modelling. The caveat however is that it requires tensor scaling and SR in the backwards pass to achieve this performance. We further find throughout our experiments that NaN-handling also depends on scale format and that although it doesn't have a big impact, it matters.

Principle 3: The Performance-Overhead Frontier is Sparse From our sweeps over thousands of configurations, we find that only a handful of techniques such as Hadamard transforms, tensor scal-

[2]This operation adds an approximate $\sim \mathcal{O}(n)$ non-fusable overhead due to additional `absmax` normalisation.

ing, stochastic rounding and optimiser choice provide a consistent, positive return on their computational overhead. We illustrate this in Pareto-frontier plots in Figure 4 for each dataset and Appendix Figure 10 for the `UE5M3` experiments. We overall observe that less complex configurations achieve better scores, and adding complexity yields diminishing returns. One can achieve lower loss, but often at a significant cost with respect to increased overhead, as observed in classification tasks.

Figure 4: Pareto-frontier plots for each dataset, $\Omega(c)$ on the x-axis and $S(c)$ on the y-axis. $S(c) = 0$ implies the configuration c matches `BFLOAT16` performance.

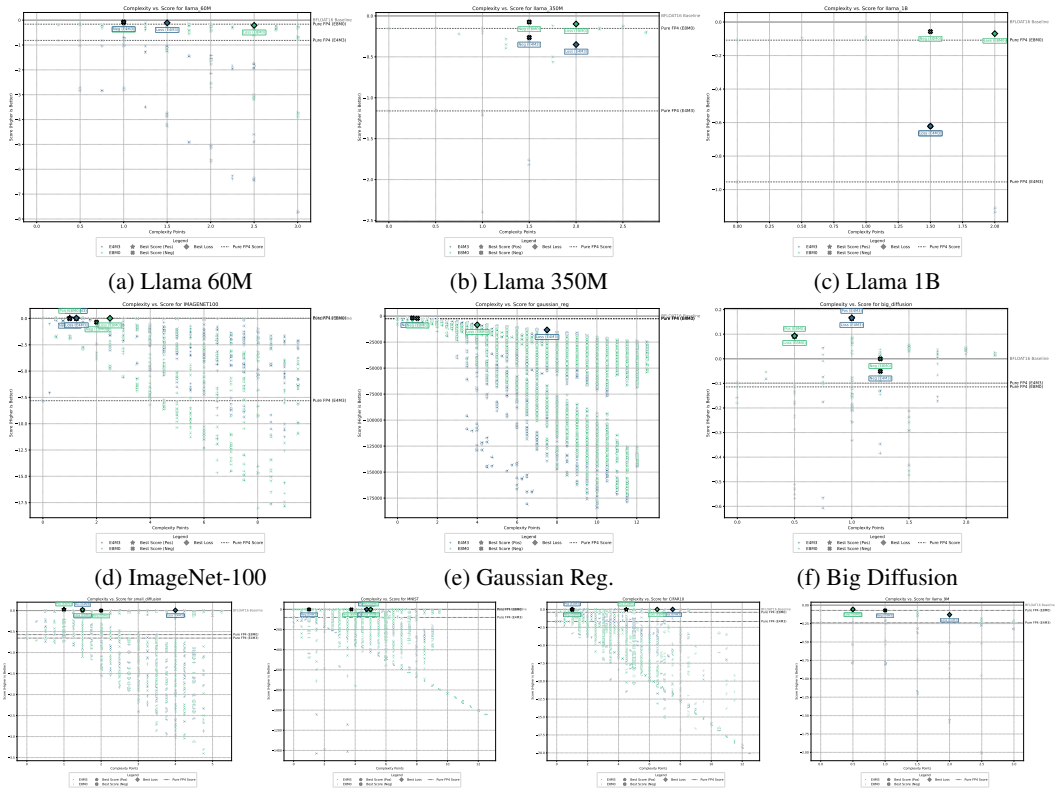

(a) Llama 60M (b) Llama 350M (c) Llama 1B

(d) ImageNet-100 (e) Gaussian Reg. (f) Big Diffusion

(g) Small Diffusion (h) MNIST (i) CIFAR-10 (j) Llama 9M

Conclusion and further work We propose a novel framework for deriving the exact gradient updates for a linear layer under micro-scaling quantisation. While differentiable `absmax` gradients and quantisation gradients provided a benefit on smaller classification tasks, we found they offered no improvement or were detrimental for larger diffusion and language models, suggesting they can often be omitted to reduce overhead without sacrificing performance in these domains. Stochastic rounding of the scale showed little success beyond small models. We further find that the range of `NVFP4` hampers its performance on language models, and that the format might require additional overhead inducing adjustments beyond what is presented in Chmiel et al. (2025) for language models up to 1B. We find that `UE5M3` scale yields better results than `MXFP4`, offering a compromise between range and precision, however requiring tensor scaling and SR to work for LLM training, introducing, albeit manageable, overhead. For further research on hardware supporting FP4 training, we'd recommend starting out with `MXFP4` and implementing fusable operations such as Hadamard transformation, SR, Tensor scaling, being mindful of NaN-handling, carefully selecting the optimiser and finally exploring different scaling formats such as `UE5M3`. Finally, our work highlights that FP4 training dynamics may not be consistent across model scales, and leave this critical direction for further research.

Reproducibility statement We provide the entire codebase in this Google Drive Link. One can use `uv` applied to the `.pytoml` file to reproduce the environment. Our code will run on commonly available hardware compatible with `PyTorch`. We've only used open-source datasets and included the download scripts in the codebase. We've ensured to fix all the seeds for all our runs (defined in the code), to hopefully provide total consistent and reproducible runs.

REFERENCES

Charlie Blake, Douglas Orr, and Carlo Luschi. Unit scaling: Out-of-the-box low-precision training, 2023. URL https://arxiv.org/abs/2303.11257.

Rishi Bommasani et al. On the opportunities and risks of foundation models, 2021. URL https://arxiv.org/abs/2108.07258.

Hengjie Cao, Mengyi Chen, Yifeng Yang, Ruijun Huang, Fang Dong, Jixian Zhou, Anrui Chen, Mingzhi Dong, Yujiang Wang, Jinlong Hou, Yuan Cheng, Fan Wu, Fan Yang, Tun Lu, Ning Gu, and Li Shang. Metis: Training large language models with advanced low-bit quantization, 2025. URL https://arxiv.org/abs/2509.00404.

Roberto L. Castro, Andrei Panferov, Soroush Tabesh, Oliver Sieberling, Jiale Chen, Mahdi Nikdan, Saleh Ashkboos, and Dan Alistarh. Quartet: Native fp4 training can be optimal for large language models, 2025. URL https://arxiv.org/abs/2505.14669.

Yuxiang Chen, Haocheng Xi, Jun Zhu, and Jianfei Chen. Oscillation-reduced mxfp4 training for vision transformers, 2025. URL https://arxiv.org/abs/2502.20853.

Brian Chmiel, Maxim Fishman, Ron Banner, and Daniel Soudry. Fp4 all the way: Fully quantized training of llms, 2025. URL https://arxiv.org/abs/2505.19115.

Eleks Corp. How llms think: Understanding the power of attention mechanisms, 2025. URL https://eleks.com/blog/how-llms-think/.

Rares Dolga et al. Latte: Latent attention for linear time transformers, 2024. URL https://arxiv.org/abs/2402.17512.

Furkan Duman-Keles et al. On the computational complexity of self-attention. 2023. arXiv preprint arXiv:2301.xxxxx.

Maxim Fishman, Brian Chmiel, Ron Banner, and Daniel Soudry. Scaling fp8 training to trillion-token llms, 2025. URL https://arxiv.org/abs/2409.12517.

Andrew Fitzgibbon and Stephen Felix. On stochastic rounding with few random bits, 2025. URL https://arxiv.org/abs/2504.20634.

Zhiwei Hao, Jianyuan Guo, Li Shen, Yong Luo, Han Hu, Guoxia Wang, Dianhai Yu, Yonggang Wen, and Dacheng Tao. Low-precision training of large language models: Methods, challenges, and opportunities, 2025. URL https://arxiv.org/abs/2505.01043.

Tianjin Huang, Haotian Hu, Zhenyu Zhang, Gaojie Jin, Xiang Li, Li Shen, Tianlong Chen, Lu Liu, Qingsong Wen, Zhangyang Wang, and Shiwei Liu. Stable-spam: How to train in 4-bit more stably than 16-bit adam, 2025. URL https://arxiv.org/abs/2502.17055.

Salman Khan, Muzammal Naseer, Munawar Hayat, Syed Waqas Zamir, Fahad Shahbaz Khan, and Mubarak Shah. Transformers in vision: A survey. *ACM Computing Surveys*, 54(10s):1–41, January 2022. ISSN 1557-7341. doi: 10.1145/3505244. URL http://dx.doi.org/10.1145/3505244.

Muyang Li, Yujun Lin, Zhekai Zhang, Tianle Cai, Xiuyu Li, Junxian Guo, Enze Xie, Chenlin Meng, Jun-Yan Zhu, and Song Han. Svdquant: Absorbing outliers by low-rank components for 4-bit diffusion models, 2025. URL https://arxiv.org/abs/2411.05007.

Paulius Micikevicius, Sharan Narang, Jonah Alben, Gregory Diamos, Erich Elsen, David Garcia, Boris Ginsburg, Michael Houston, Oleksii Kuchaiev, Ganesh Venkatesh, and Hao Wu. Mixed precision training, 2018. URL https://arxiv.org/abs/1710.03740.

Paulius Micikevicius, Dusan Stosic, Neil Burgess, Marius Cornea, Pradeep Dubey, Richard Grisenthwaite, Sangwon Ha, Alexander Heinecke, Patrick Judd, John Kamalu, Naveen Mellempudi, Stuart Oberman, Mohammad Shoeybi, Michael Siu, and Hao Wu. Fp8 formats for deep learning, 2022. URL https://arxiv.org/abs/2209.05433.

Asit Mishra, Dusan Stosic, and Simon Layton. Recipes for pre-training llms with mxfp8, 2025. URL https://arxiv.org/abs/2506.08027.

Badreddine Noune, Philip Jones, Daniel Justus, Dominic Masters, and Carlo Luschi. 8-bit numerical formats for deep neural networks, 2022. URL https://arxiv.org/abs/2206.02915.

Houwen Peng, Kan Wu, Yixuan Wei, Guoshuai Zhao, Yuxiang Yang, Ze Liu, Yifan Xiong, Ziyue Yang, Bolin Ni, Jingcheng Hu, Ruihang Li, Miaosen Zhang, Chen Li, Jia Ning, Ruizhe Wang, Zheng Zhang, Shuguang Liu, Joe Chau, Han Hu, and Peng Cheng. Fp8-lm: Training fp8 large language models, 2023. URL https://arxiv.org/abs/2310.18313.

Bita Darvish Rouhani, Ritchie Zhao, Ankit More, Mathew Hall, Alireza Khodamoradi, Summer Deng, Dhruv Choudhary, Marius Cornea, Eric Dellinger, Kristof Denolf, Stosic Dusan, Venmugil Elango, Maximilian Golub, Alexander Heinecke, Phil James-Roxby, Dharmesh Jani, Gaurav Kolhe, Martin Langhammer, Ada Li, Levi Melnick, Maral Mesmakhosroshahi, Andres Rodriguez, Michael Schulte, Rasoul Shafipour, Lei Shao, Michael Siu, Pradeep Dubey, Paulius Micikevicius, Maxim Naumov, Colin Verrilli, Ralph Wittig, Doug Burger, and Eric Chung. Microscaling data formats for deep learning, 2023. URL https://arxiv.org/abs/2310.10537.

Huangyuan Su, Mujin Kwun, Stephanie Gil, Sham Kakade, and Nikhil Anand. Characterization and mitigation of training instabilities in microscaling formats, 2025. URL https://arxiv.org/abs/2506.20752.

Xiao Sun, Jungwook Choi, Chia-Yu Chen, Naigang Wang, Swagath Venkataramani, Vijayalakshmi (Viji) Srinivasan, Xiaodong Cui, Wei Zhang, and Kailash Gopalakrishnan. Hybrid 8-bit floating point (hfp8) training and inference for deep neural networks. In H. Wallach, H. Larochelle, A. Beygelzimer, F. d'Alché-Buc, E. Fox, and R. Garnett (eds.), *Advances in Neural Information Processing Systems*, volume 32. Curran Associates, Inc., 2019. URL https://proceedings.neurips.cc/paper_files/paper/2019/file/65fc9fb4897a89789352e211ca2d398f-Paper.pdf.

Albert Tseng, Jerry Chee, Qingyao Sun, Volodymyr Kuleshov, and Christopher De Sa. Quip#: Even better llm quantization with hadamard incoherence and lattice codebooks, 2024. URL https://arxiv.org/abs/2402.04396.

Albert Tseng, Tao Yu, and Youngsuk Park. Training llms with mxfp4, 2025. URL https://arxiv.org/abs/2502.20586.

Ashish Vaswani et al. Attention is all you need. In *Advances in Neural Information Processing Systems*, 2017.

Ruizhe Wang, Yeyun Gong, Xiao Liu, Guoshuai Zhao, Ziyue Yang, Baining Guo, Zhengjun Zha, and Peng Cheng. Optimizing large language model training using fp4 quantization, 2025. URL https://arxiv.org/abs/2501.17116.

Hanmei Yang, Summer Deng, Amit Nagpal, Maxim Naumov, Mohammad Janani, Tongping Liu, and Hui Guan. An Empirical Study of Microscaling Formats for Low-Precision LLM Training . In *2025 IEEE 32nd Symposium on Computer Arithmetic (ARITH)*, pp. 1–8, Los Alamitos, CA, USA, May 2025. IEEE Computer Society. doi: 10.1109/ARITH64983.2025.00011. URL https://doi.ieeecomputersociety.org/10.1109/ARITH64983.2025.00011.

Jiecheng Zhou, Ding Tang, Rong Fu, Boni Hu, Haoran Xu, Yi Wang, Zhilin Pei, Zhongling Su, Liang Liu, Xingcheng Zhang, and Weiming Zhang. Towards efficient pre-training: Exploring fp4 precision in large language models, 2025. URL https://arxiv.org/abs/2502.11458.